



HAL
open science

Experimental and numerical study of the fuel effect on flame propagation in long open tubes

Guillaume Lecocq, Jérôme Daubech, Emmanuel Leprette

► To cite this version:

Guillaume Lecocq, Jérôme Daubech, Emmanuel Leprette. Experimental and numerical study of the fuel effect on flame propagation in long open tubes. 14th International Symposium on Hazards, Prevention, and Mitigation of Industrial Explosions (ISHPMIE 2022), Jul 2022, Braunschweig, Germany. pp.721-731, 10.7795/810.20221124 . ineris-03975648

HAL Id: ineris-03975648

<https://ineris.hal.science/ineris-03975648>

Submitted on 17 Apr 2023

HAL is a multi-disciplinary open access archive for the deposit and dissemination of scientific research documents, whether they are published or not. The documents may come from teaching and research institutions in France or abroad, or from public or private research centers.

L'archive ouverte pluridisciplinaire **HAL**, est destinée au dépôt et à la diffusion de documents scientifiques de niveau recherche, publiés ou non, émanant des établissements d'enseignement et de recherche français ou étrangers, des laboratoires publics ou privés.

Experimental and numerical study of the fuel effect on flame propagation in long open tubes

Guillaume Lecocq^a, Jérôme Daubech^a & Emmanuel Leprette^a

Institut National de l'Environnement Industriel et des Risques, Parc Technologique ALATA, BP 2,
60550 Verneuil-en-Halatte, France

E-mail: guillaume.lecocq@ineris.fr

Abstract

Previous works (Daubech, Lecocq, 2019) were dedicated to gaseous flame acceleration along long pipes with a set of cases studied both experimentally and numerically. In these cases, the flammable mixture was initially quiescent and homogeneously distributed. The impact of the tube diameter and material were studied through both approaches for rather slow flames, the fuel being methane. While main features of the real flame were recovered by the chosen CFD method, some limits remained.

A new experimental dataset is detailed and analyzed with a quicker flame, the fuel being hydrogen and the same experimental set-up as the one used for measuring slow flames. Thus, the fuel effect on the flame dynamics can be directly highlighted.

A simple CFD approach is tested for recovering two distinct flame behaviors: a deflagration flame and another undergoing deflagration-to-detonation transition. Furthermore, the modelling results are used to propose elements of interpretation for flame acceleration.

Keywords: *premixed gaseous flame propagation, hydrogen, methane, pipes, CFD*

1. Introduction

Scenarios of formation of gaseous flammable clouds in long ducts can be identified during risk analyses of industrial processes. If an ignition occurs, a flame can propagate in such flammable cloud and undergo an acceleration which is specific to this confined and elongated geometry.

If the flammable cloud formation and the ignition cannot be avoided, it is key to assess the flame acceleration process and the generated pressure effects associated to the explosion scenario. These latter should be compared to the mechanical resistance properties of the pipe in which the explosion could be triggered. To do so, the flame acceleration process has to be understood with the specificities of the explosion scenario (tube material and diameter, flammable cloud length, spatial distribution of the fuel in this cloud, ...).

Previous experimental and numerical works were detailed for 24 m long pipes made of PMMA or steel, with varying diameters (150 or 250 mm), the fuel being methane (Daubech, Lecocq, 2019). The pipes were open at one end and closed at the other where ignition was triggered. The tests showed the impact of the pipe material and diameter.

In the current work, new experimental data are presented. They correspond to the case of a 150 mm wide steel tube in which a homogeneous hydrogen/air cloud with a volume fraction of 20 % is ignited. They are compared to another experimental point for which the flammable cloud is made of a stoichiometric methane/air cloud.

A CFD approach is proposed and tested, in order to assess its predictive capacities and study if elements could be extracted from computations for helping to interpret experiments.

2. Experimental set-up and results

The current work is dedicated to flames propagating in a straight, 24-m long steel pipe, open at one end and closed at the other. It is filled with a quiescent stoichiometric methane/air mixture. Ignition is performed on the middle of the closed end with an electrical spark whose energy is about 100 mJ.

Two flammable mixtures are studied:

- A stoichiometric methane/air mixture,
- A lean hydrogen/air mixture, with a hydrogen volume fraction in air of 20 %.

Figure 1 shows the pipe in which flame propagation is measured.



Fig. 1. *View of the experimental set-up. Steel pipe, with a 150-mm inner diameter.*

The flame position is tracked with four photovoltaic cells located at 0.5 m, 5.5 m (4.5 m for methane), 10.5 m and 15.5 m from ignition point. Pressure signals are measured with three probes close to ignition point and at 5 m and 15.5 m from ignition point.

More details about the experimental set-up are given of the paper of Daubech (2019).

Raw experimental results the flame trajectory and pressure signals are given in Figures 2-3 and Figures 6-7 for both fuels. Two different behaviors can be noticed.

For the methane/air flame, while the flame speed keeps on increasing, its maximum value remains about 140 m/s. Two main peaks can be seen for each pressure signal.

The first one can be explained with flame elongation that follows ignition, which leads to an increase of the burnt gases volume variation per time unit. When this variation becomes weaker, because a maximum in flame surface is reached, the pressure decays. The flame continues to accelerate, eventually with a change in flame shape, and the volume production of burnt gases creates the second peak which is limited by the amount of flammable mixture in the tube. A maximum overpressure about 400 mbar is reached. The time needed to burn all the flammable mixture is between 0.25 s and 0.3 s.

For the hydrogen/air flame also, a continuous flame acceleration can be noticed. A maximum flame speed higher than 2000 m/s is measured. This value can be compared to the Chapman-Jouguet velocity, about 1710 m/s. In this case, a transition from a deflagration regime to a detonation one (DDT) is observed.

At the pressure probe located 5.5 m away from ignition point, a first peak similar to the first peak identified for the methane/air flame appears. A slight pressure decay then occurs and is followed by

a continuous pressure increase until a maximum overpressure of 3 bar. 15.5 m away from ignition point, a shock wave appears with a peak about 20 bar. This value is higher than the Chapman-Jouguet pressure (13 bar), which, additionally to what was said for flame velocity, indicates an overdriven detonation.

3. Phenomenology related to explosions in pipes and CFD modelling

3.1 Phenomenology

Cicarelli et al. (2008) proposed a review article dedicated to flame acceleration in pipes. With ignition, a burnt gases kernel is created, which leads to the formation of a premixed laminar flame. It is first wrinkled due to Darrieus-Landau instability, which is promoted or counteracted by thermo-diffusive effects, respectively if the Lewis number is lower or higher than 1. In the same time, the fresh gases are pushed ahead of the flame front due to thermal expansion effects. The flame front then reaches the lateral wall of the tube, leading to slight deceleration of the burnt gases production, the flame surface being reduced. It can be also promoted by heat losses, depending on the tube material. After this initial stage, the flame keeps on propagating with a shape that can sequentially change from an elongated flame to a tulip-shape flame, still pushing the fresh gases. The flame acceleration mechanism in this phase remains discussed.

With his pioneer works, Shchelkin (1940, 1965) explained flame self-acceleration in tubes with flame/turbulence interaction, turbulence being produced in the fresh gases after generation of a boundary layer on the walls. This explanation highlights the importance of the wall roughness on the flame dynamics. Experiments (Daubech, 2019) carried out for methane/air flames propagating in long open tubes with different materials (ie PMMA for a smooth tube and steel for a rough tube) indeed led to different flame dynamics provided the tube diameter was small enough. The same set of experiments also showed the wall turbulence remained limited at the walls for the widest tubes while flame acceleration was noticed.

According to Cicarelli et al. (2008), a detonation can be first initiated after a shock reflection or a shock focusing. The shock is strong enough to auto-ignite fresh gases and trigger detonation. It can also be due to more subtle mechanisms involving instabilities and mixing processes. These phenomena were first explained by Zeldovitch (1970) and Lee (1978): if an induction time gradient is formed, due to local inhomogeneities (temperature and/or concentration). The related spontaneous flame would release heat and create a shock wave. If the heat release strengthens the shock wave sufficiently, a detonation can occur. More recent works (Ivanov, 2011) called into question this mechanism. According to the authors, DDT occurs when the flame is so fast that formed shock waves sit on the flame front and a coupling mechanism leads to a sufficient increase of flame speed and pressure peak.

3.2 Modelling approaches available in the literature

CFD approaches available in the literature for flame acceleration in tubes rely either on a highly detailed description of the flow (Oran, 2007) or “under resolved” modelling that are built with numerous sub-models, each one accounting for a physical feature (Wieland, 2021).

With such models, the chemical source term which pilots the propagation speed of the flame front is simply closed as the product of the gradient of the progress variable (\tilde{c}), the volume mass of the fresh gases (ρ^u) and a characteristic flame speed: $\bar{\rho} \tilde{\omega}_c = \rho^u S_F |\nabla \tilde{c}|$. The flame speed S_F then writes: $\Xi \cdot S_L$ where Ξ is a wrinkling factor. This latter is explained as the product of characteristic wrinkling factors, each one accounting for a phenomenon accelerating the flame speed: thermo-diffusive and Darrieus-Landau instabilities, pressure effects, ...

Some authors (Wieland, 2021, Bradley, 2012) describe detonation as the coupling of auto-ignition of fresh gases coupled to the propagation of a shock wave. Chemical source terms can be built from two contributions (Lecocq, 2011, Wieland, 2021): one modelling a premixed flame, the other auto-ignition, in order to account for the transition between the deflagration and the detonation.

3.3 Approach retained

The computations presented in the current work are based on a modelling strategy close to the one of Wieland (2021) for modelling deflagrations. The transport equations are solved for momentum, pressure, a progress variable and energy with a pressure-based solver of the CFD code OpenFoam v2106 (Weller, 1998). Turbulence is also modelled with a $k-\omega$ SST model (Menter, 2003).

Concerning the methane/air flame the pressure effects remain moderate. A constant laminar flame speed of 0.4 m/s was used. The pressure effects are well higher for the hydrogen/air flame and they have to be included for the estimation of the fresh gases volume mass ρ^u and the laminar flame speed S_L . ρ^u is simply quantified under the assumption of an adiabatic compression, thanks to the pressure field. Correlations can be found in the literature for the laminar flame speed of hydrogen. Nevertheless, it is not clear according to bibliography if laminar flame speed should increase or decrease with pressure (Bougrine, 2011, Salzano, 2012). Then, for the sake of simplicity, a constant laminar flame speed value of 0.9 m/s is used for the hydrogen flame.

The wrinkling factor Ξ is closed as: $\Xi = \Xi_t \cdot \Xi_I$ where Ξ_t represent flame wrinkling induced by flame/turbulence interaction and is closed with the turbulent flame speed correlation proposed by Gülder (1991). The wrinkling factor Ξ_I represents the effects of instabilities. The commonly made assumption of a unitary Lewis number for methane/air flames is kept and Ξ_I is set to 1.0 in this case. Concerning the hydrogen/air flame, its Lewis number, about 0.6, is smaller than 1.0 and instabilities at the flame front are expected. A value for Ξ_I remains hard to predict. An ad hoc way was to tune it in order to recover a proper flame trajectory with time. A constant value of 3.3 was identified.

The computational domain is limited to the part of the pipe filled by the flammable mixture. At walls, velocity is zero and turbulent viscosity is modelled with a wall law. At the outlet plane, the pressure is set to the atmospheric pressure and the velocity gradient is set to 0.

The walls are assumed to be adiabatic (temperature gradient set to 0). The steel roughness is assumed to be around 150 μm which corresponds to a weakly rusted steel. This characteristic is used in the wall laws.

The mesh is made of 2.5 million hexahedra. The maximum characteristic cell width is about 6 mm. The cells are refined at the walls.

4. Results

According to Figure 2, the computation enabled to recover a qualitative agreement for the evolution of the flame front position with time. The increase in flame velocity is satisfying from $t=0\text{s}$ to $t=0.05\text{ s}$ and from $t=0.15\text{ s}$ to $t=0.25\text{ s}$ but is overpredicted from $t=0.05\text{ s}$ to $t=0.15\text{ s}$.

Figure 3 shows the main features of the pressure signals are predicted. At 5.5 m and 10.5 m, there is a first pressure peak, followed by a pressure decay and one or several peaks. The amplitude of the first pressure peak is about 200 mbar and the second is about 400 mbar. The overestimation of the first peak by the modelling is about 25 % while the second one ranges from 25 to 50 %.

It is interesting to go a little bit further in the computation post-processing as several quantities can explain pressure effects. Indeed, these latter are related to the volume rate at which burnt gases are produced by flame propagation, the tube acoustics and the effect of the opening.

The total flame surface captured by the mesh is quantified as: $S_{res} = \int_V |\nabla \tilde{c}| dV$. A resolved wrinkling, Ξ_{res} , can be defined as the ratio of this surface to the tube section. The turbulent wrinkling averaged on the flame surface, $\langle \Xi_t \rangle_s$ is also computed. The evolution of these quantities with time is plotted in Figure 4.

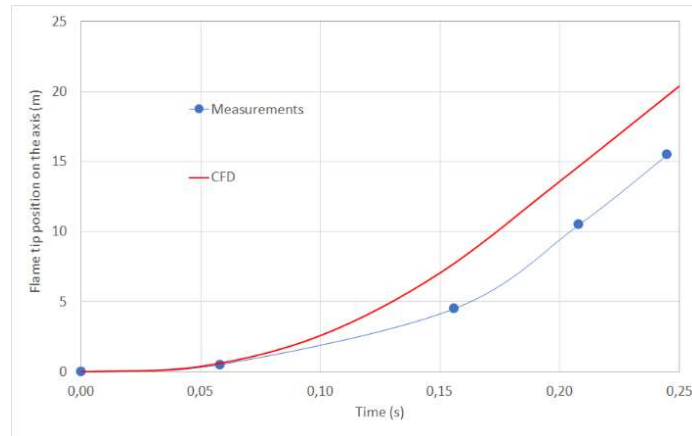


Fig. 2. Experimental and computed flame trajectory on the axis for the methane/air flame.

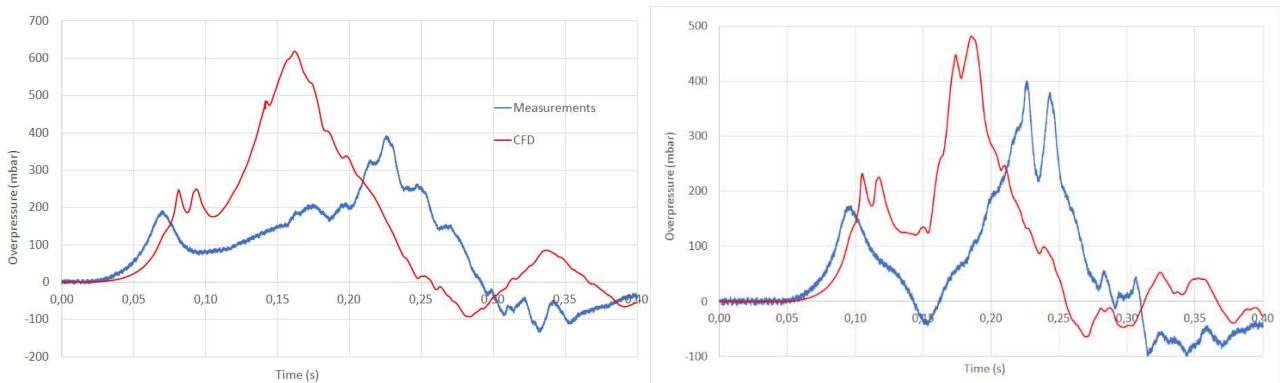


Fig. 3. Experimental and computed pressure signals at 5.5 m (left) and 15.5 m (right) from ignition point for the methane/air flame.

$\langle \Xi_t \rangle_s$ mainly increases with time, starting from $t=0.05$ s. The final value reached is about 15. Ξ_{res} does not follow the same evolution: there are two cycles of increase/decrease and a constant value is observed for the final propagation phase. The maximum value is about 8. According to the Figure 5,

the maximum values, reached for example at $t=0.05$ s and $t=0.15$ s correspond to elongated flames. The lowest values at the end of flame propagation are obtained for quasi-flat flames.

It is notably interesting to note that:

- the first pressure peak at 0.07 s seems to be mainly explained by flame elongation and very weak flame/turbulence interaction,
- the pressure decay that follows is related to the change of the flame shape (from an elongated shape to a tulip shape),
- the pressure peak at 0.15 s is obtained when the product $\langle \Xi_t \rangle_s \cdot \Xi_{res}$ is the highest.

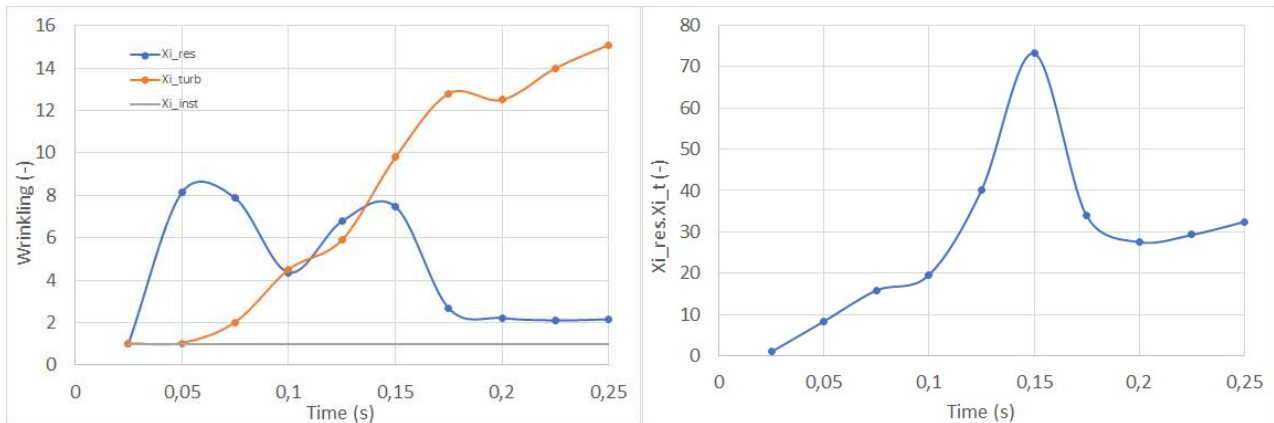


Fig. 4. Evolution of characteristic wrinkling factors for the methane/air flame with time (left) and of the products of all wrinkling factors (right)

Figure 6 shows the experimental and predicted flame trajectory. It should be recalled here that the parameter Ξ_t was adjusted to recover a satisfying flame trajectory.

Figure 7 highlights the main trends of the pressure signals were recovered. At 5.5 m, the computed pressure signal is characterized with three peaks, with an overall pressure increase. The amplitude of the pressure is closed to the measured one. 15.5 m away from ignition point, the measured shock wave is predicted, nevertheless with a peak overestimation of 75 %. This proves a pressure-based solver is able to deal with shocks. Other authors choose to change their solver when the flame velocity exceeds a critical value (Wieland, 2021).

The characteristic wrinkling factors are also plot for the hydrogen flame (Figure 8). $\langle \Xi_t \rangle_s$ mainly increases, starting from 0.01 s to 0.06 s and then decreases. The peak value is very high (85 *ie* about 6 times the peak value observed for the methane/air flame). As for the methane/air flame, Ξ_{res} sequentially increases and decreases. The peak values of lower than those obtained for the methane/air flame.

The first pressure peak seems to be explained by an increased flame surface as well as flame instabilities. A pressure decay is observed, related to a rapid change of the flame shape which is not compensated by flame instabilities and flame/turbulence interaction. After this phase, while the flame shape and surface evolve (Figure 9), the flame acceleration is mainly promoted by flame/turbulence interaction, until the end of the flame propagation in the tube.

Here DDT was approached through a continuous turbulent flame acceleration until the flame front reaches the preceding shock wave. This point of view is closed to the Shchelkin one but it may be too much simple compared to realistic mechanisms. It is indeed possible that the CFD model should predict flame extinction instead of flame acceleration.

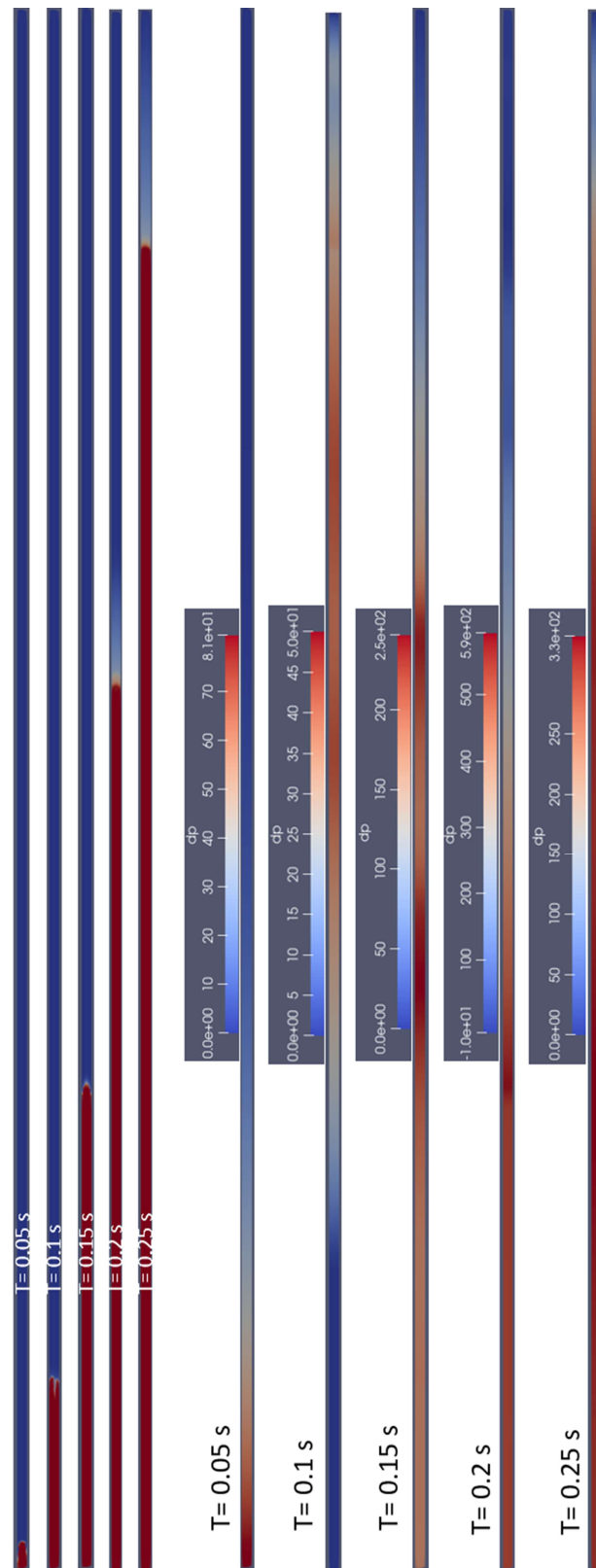


Fig. 5. Evolution with time of the flame (left) and of the pressure field (right) for the computed methane/air flame. Units for pressure are mbar.

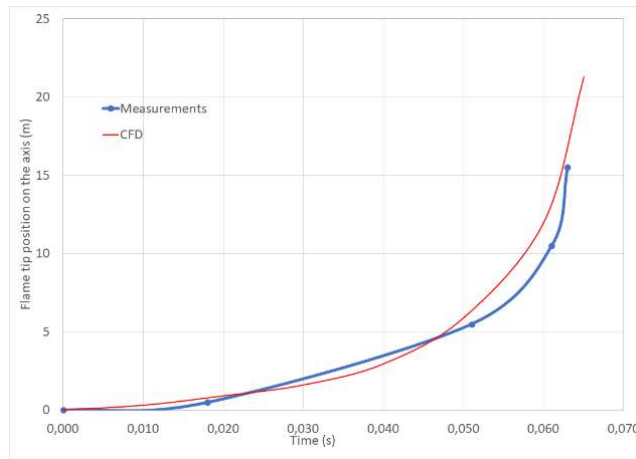


Fig. 6. Experimental and computed flame trajectory on the axis for the hydrogen/air flame

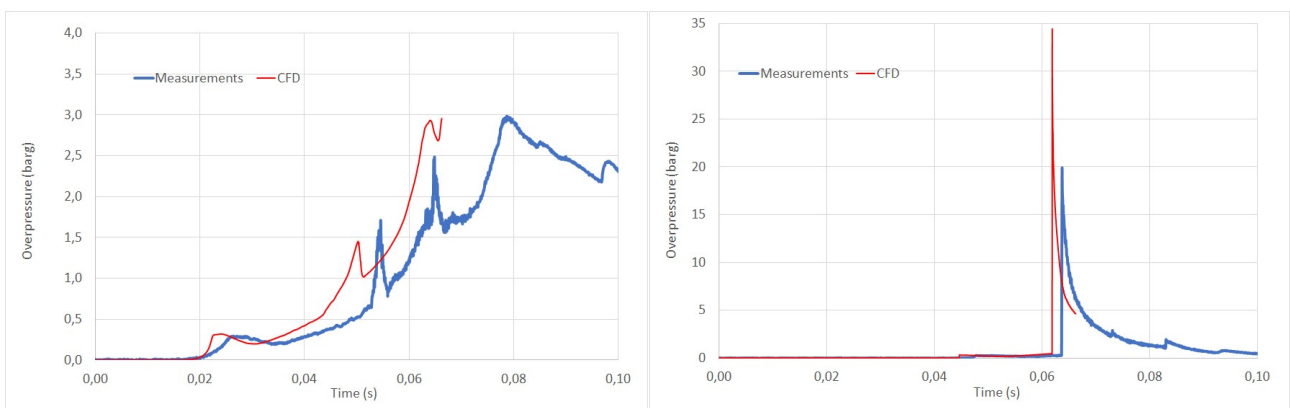


Fig. 7. Experimental and computed pressure signals at 5.5 m (left) and 15.5 m (right) from ignition point for the hydrogen/air flame.

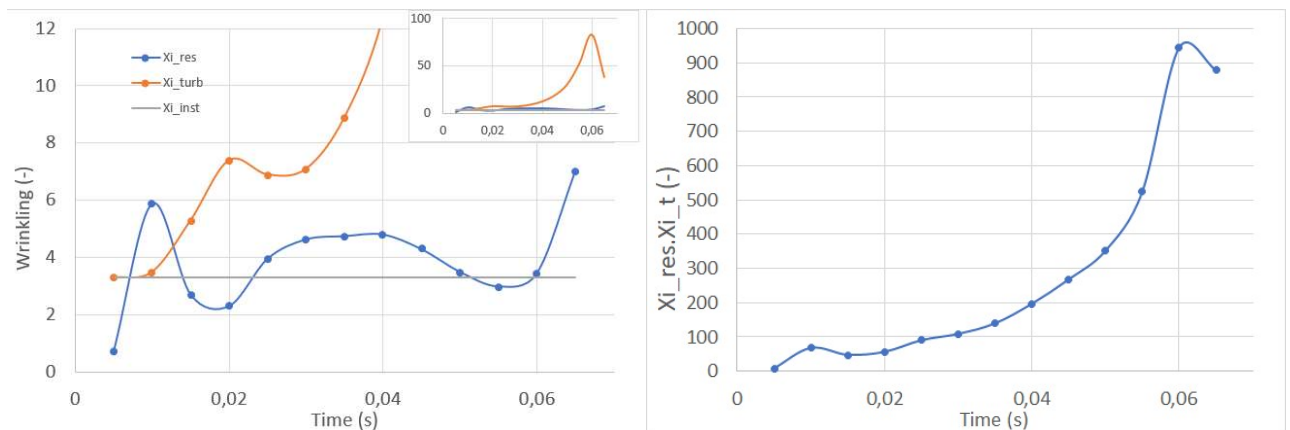


Fig. 8. Evolution of characteristic wrinkling factors for the hydrogen/air flame with time (left) and of the products of all wrinkling factors (right)

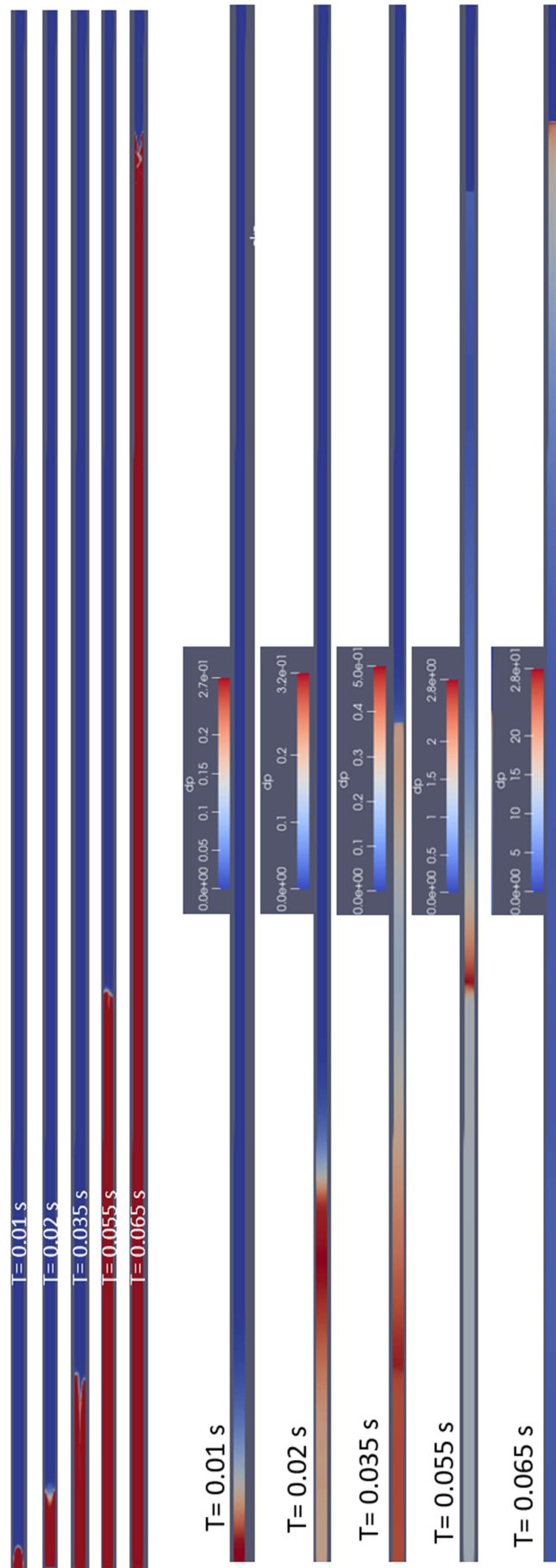


Fig. 9. Evolution with time of the flame (left) and of the pressure field (right) for the computed hydrogen/air flame. Units for pressure are bar.

5. Conclusions

Experimental results were first shown for a 24 m long steel pipe in which initially quiescent flammable mixtures were ignited, one being a stoichiometric methane/air mixture, the other a lean hydrogen/air mixture.

Two distinct flame behaviours were observed: the maximum propagation speed of the methane/air flame was about 140 m/s while DDT occurred for the hydrogen/air flame.

A simple CFD model was used to recover features of both cases. An agreement was found for flame position with time and pressure effects.

The raw CFD results were post-processed to give pieces of interpretation for what was observed. One interest of CFD here is to give access to more quantities than the measured ones. Thus, it was possible to study the effect of turbulence, instabilities and flame shape changes on the pressure effects.

Nevertheless, the current CFD model should be completed with other sub-models (extinction, autoignition sub-models, ...) as it is possible that the acceleration for the hydrogen flame, numerically explained by flame/turbulence interaction is not as large as predicted.

References

- Daubech, J., Proust, C., Leprette, E., Lecocq, G. (2019). Further insight into the gas flame acceleration mechanisms in pipes. Part I: experimental work. *Journal of Loss Prevention in the Process Industries* 62, 103930
- Lecocq, G., Leprette, E., Daubech, J., Proust, C. (2019). Further insight into the gas flame acceleration mechanisms in pipes. Part II: numerical work. *Journal of Loss Prevention in the Process Industries* 62, 103919
- Cicarelli G. and Dorofeev S. (2008) Flame acceleration and transition to detonation in ducts. *Progress in Energy and Combustion Science* 34, pp. 499-550
- Shchelkin KI (1940) Influence of the wall roughness on initiation and propagation of detonation in gases. *Zh Eksp Teor Fiz* 10, pp. 823-827.
- Shchelkin KI, Troshin YaK (1965) *Gas dynamics of combustion*. Baltimore: Mono book corp.
- Zeldovitch YaB, Librovich VB, Makhiviladze GM. Sivanshinsky GI (1970) On the development of detonation in a non-uniformly preheated gas. *Astronautica Acta* 15, pp. 313-321
- Lee JHS, Knystautas R, Yoshikawa N (1978) Photochemical initiation and gaseous detonations. *Acta Astronautica* 5, pp. 971-972
- Ivanov M.F., Kiverin A.D., Liberman M.A. (2011) Flame acceleration and DDT of hydrogen-oxygen gaseous mixtures in channels with no-slip walls. *Int. J. of Hydrogen Energy* 36, pp. 7714-7727
- Lecocq G., Richard S., Michel J.-B., Vervisch L. A new LES model coupling flame surface density and tabulated kinetics approaches to investigate knock and pre-ignition in piston engines, *Proceedings of the Combustion Institute* 33(2) (2011) 3105-3114
- Oran E.S., Gamezo E.N. (2007) Origins of the deflagration-to-detonation transition in gas-phase combustion. *Combust. Flame* 148, pp. 4-47
- Wieland C., Scharf F., Shildberg H.-P., Hoferichter V., Eble J., Hirsch C., Sattelmayer T. (2021) Efficient simulation of flame acceleration and deflagration-to-detonation transition in smooth pipes. *Journal of Loss Prevention in the Process Industries* 71, 104504
- Bradley D (2012) Autoignitions and detonations in engines and ducts, *Phil. Trans. R. Soc. A* (2012) 370, 689–714
- Weller, H.G, Tabor, G. (1998). A tensorial approach to computational continuum mechanics using object-oriented techniques. *Computational Physics*, 12: 620-631.

- Menter F.R., Kuntz M., and Langtry R. (2003). Ten years of industrial experience with the SST turbulence model. *Proceedings of the international symposium on turbulence, heat and mass transfer*, 4: 625–632.
- Gülder O. (1991) Turbulent premixed flame propagation models for different combustion regimes. *Proc. Combust. Inst.* 23, pp. 743-750
- Bougrine S. et al. (2011) Numerical study of laminar flame properties of diluted methane-hydrogen-air flames at high pressure and temperature using detailed chemistry. *Int. Journal of Hydrogen Energy* 36, pp 12035-12047
- Salzano E. et al. (2012) Explosion behavior of hydrogen-methane/air mixtures. *J. Loss Prev. In the Process Ind.* 25, pp. 443-447